

---

# DICTIONARY-LEARNING-BASED DATA PRUNING FOR SYSTEM IDENTIFICATION

---

A PREPRINT

Tingna Wang<sup>† \*1,3</sup>, Sikai Zhang<sup>†2</sup>, and Limin Sun<sup>1,3,4</sup>

<sup>1</sup>Department of Bridge Engineering, Tongji University, Shanghai, China

<sup>2</sup>Baosight Software

<sup>3</sup>Shanghai Qi Zhi Institute, Shanghai, China

<sup>4</sup>State Key Laboratory of Disaster Reduction in Civil Engineering, Tongji University, Shanghai, China

February 18, 2025

## ABSTRACT

System identification is normally involved in augmenting time series data by time shifting and non-linearisation (via polynomial basis), which introduce redundancy both feature-wise and sample-wise. Many research works focus on reducing redundancy feature-wise, while less attention is paid to sample-wise redundancy. This paper proposes a novel data pruning method, called (mini-batch) FastCan, to reduce sample-wise redundancy based on dictionary learning. Time series data is represented by some representative samples, called atoms, via dictionary learning. The useful samples are selected based on their correlation with the atoms. The method is tested on one simulated dataset and two benchmark datasets. The R-squared between the coefficients of models trained on the full and the coefficients of models trained on pruned datasets is adopted to evaluate the performance of data pruning methods. It is found that the proposed method significantly outperforms the random pruning method.

## 1 Introduction

System identification refers to a method of identifying the mathematical description of a dynamic system using measured input-output data [1]. It can be used to forecast future values, assess the effects of input variations, design control schemes, etc. According to the objective of system identification, it can be generally divided into two types [2]. The first type focuses on the approximation scheme that produces the minimum production errors, such as fuzzy logic [3] and neural networks [4]. The second type focuses on the elucidation of the underlying rule that represents the system, such as spectral analysis [5], the Volterra series [6] and Nonlinear Auto-Regressive with eXogenous Inputs (NARX) [7]. NARX-based methods have gained increasing attention in various fields such as engineering, finance, biology, and social sciences due to their flexibility in modelling a variety of systems while maintaining interpretability [8, 2, 9].

To avoid model overfitting and reduce computational complexity, feature selection methods based on orthogonalisation techniques and greedy search are widely applied in constructing NARX models [10, 11, 12]. The orthogonalisation-based method was firstly derived in [10] to efficiently decide which terms should be included in the Nonlinear Autoregressive Moving Average with eXogenous input (NARMAX) models. Then this method was further developed in [11] as orthogonal forward-regression estimators to identify parsimonious models of structure-unknown systems by modifying and augmenting some orthogonal least squares methods. A more comprehensive review of this feature selection idea and its development for system identification can be found in [12].

Similar to feature selection, input selection is also a crucial step in system identification, which can help to improve the identification performance and reduce storage and training costs [13, 14, 12]. While optimal input selection (often referred to as data pruning) is currently an active research topic for computer vision [15, 16, 17] and natural

---

\*Corresponding author. tina.wang@tongji.edu.cn

<sup>†</sup>Equal contribution

language processing [18, 19], its application to system identification has received less attention, although it remains an intractable task.

This paper proposes a data-pruning method based on dictionary learning to select useful time series samples for constructing the simplest mathematical model to represent a system. Specifically, the reduced polynomial NARX method is applied to the identification of nonlinear dynamic systems as an example. The canonical-correlation-based fast feature selection method introduced in [20] is adopted to find the most important terms that should be included in the NARX model to achieve the required accuracy. Dictionary learning is then creatively combined with the fast feature selection method based on canonical correlation to find the most useful time series samples to train these terms.

Dictionary learning, initially popular in the signal processing area, is used to learn an overcomplete dictionary composed of signal atoms, where a sparse linear combination of these atoms can generate the original signal [21]. It is currently widely studied for image processing since images usually admit sparse representation [22, 23]. For the proposed method, k-means-based dictionary learning provides an overcomplete dictionary of time terms, which are used as pseudo-labels in the data pruning process.

In this paper, the proposed method, i.e., (mini-batch) FastCan, is compared with the random pruning method. The reduced NARX trained with the full dataset is used as the baseline model. The coefficients learned with the pruned dataset is compared with the baseline model. The more the coefficients are close to the baseline model, the better the pruned dataset is. The procedural of the research in this paper is illustrated in Fig. 1.

The next section introduces the details of the proposed data-pruning method for system identification, followed by numerical case studies to demonstrate the necessity and advantages of the method. Subsequently, case studies on two benchmark datasets for nonlinear system identification are presented, with a discussion on the effect of hyper-parameters in the proposed method. It is worth noting that the proposed method can also be used to select informative samples for general machine-learning tasks.

## 2 Methodology

This section introduces the dictionary learning-based data pruning method for a discrete system with finite orders.

### 2.1 Reduced polynomial NARX

A NARX model is used to simulate a system, which is formulated as

$$\begin{aligned} y(k) = & F[y(k-1), y(k-2), \dots, y(k-n_y), \\ & u(k-d), y(k-d-1), \dots, y(k-d-n_u)] + e(k) \end{aligned} \quad (1)$$

where  $y(k)$ ,  $u(k)$  and  $e(k)$  are the system output, input and noise sequences, respectively.  $n_y$  and  $n_u$  are the maximum terms for the system output and input.  $d$  is the time delay, typically set to  $d = 1$ .  $F[\cdot]$  is a nonlinear function.

The power-form polynomial model is adopted to approximate the nonlinear mapping  $F[\cdot]$ , and the equation (1) is then given as,

$$\begin{aligned} y(k) = & \theta_0 + \sum_{i_1=1}^n f_{i_1}(x_{i_1}(k)) \\ & + \sum_{i_1=1}^n \sum_{i_2=i_1}^n f_{i_1 i_2}(x_{i_1}(k), x_{i_2}(k)) + \dots + \sum_{i_1=1}^n \dots \\ & \sum_{i_\ell=i_{\ell-1}}^n f_{i_1 i_2 \dots i_\ell}(x_{i_1}(k), x_{i_2}(k), \dots, x_{i_\ell}(k)) + e(k) \end{aligned} \quad (2)$$

where  $\ell$  is the degree of polynomial nonlinearity,  $n = n_y + n_u$ , and

$$\begin{aligned} f_{i_1 i_2 \dots i_m}(x_{i_1}(k), x_{i_2}(k), \dots, x_{i_m}(k)) &= \theta_{i_1 i_2 \dots i_m} \prod_{k=1}^m x_{i_k}(k), \\ x_m(k) &= \begin{cases} y(k-m), & 1 \leq m \leq n_y, \\ u(k-m+n_y), & n_y+1 \leq m \leq n = n_y+n_u, \end{cases} \end{aligned}$$

<sup>2</sup>The colour style used this figure is from `bg-mp1-stylesheets` [24].

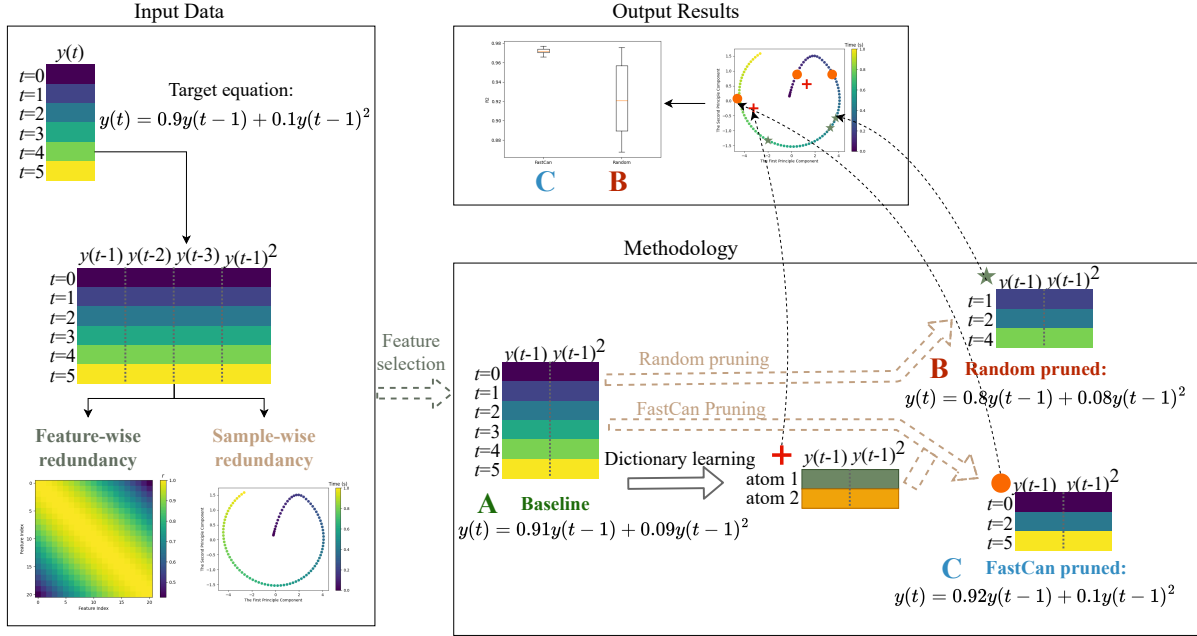


Figure 1: The schematic diagram of this research. The time series  $y(t)$  is generated by the target equation, then time-shifted and nonlinearised to construct a redundant term library. Feature-wise redundancy is represented by a correlation heatmap, while sample-wise redundancy is visualised by a principle component analysis (PCA) plot. Feature selection is applied to the term library to reduce feature-wise redundancy. **Dataset A**<sup>2</sup>, which contains the full set of samples, is used to train the **Baseline model**. **Dataset B**, a random subset of Dataset A, is used to train the **Random pruned model**. **Dataset C**, consisting of samples selected based on the atoms learned from Dataset A, is used to train the **FastCan pruned model**. The FastCan pruned dataset generally exhibits less sample-wise redundancy compared to the randomly pruned dataset, as illustrated in the PCA plot, where the data selected by FastCan are more widely spread, while the randomly pruned data tend to be close to each other. To compare the data pruning methods, Dataset A is pruned repeatedly by random selection and FastCan, and the models are then trained on the pruned datasets, respectively. The results show that the coefficients learned from the FastCan pruned data are closer to those of the baseline model, with less variance across repeated tests.

where  $1 \leq m \leq \ell$ ,  $\theta_{i_1 i_2 \dots i_m}$  are model parameters, and  $\prod_{k=1}^m x_{i_k}(k)$  are model terms whose order is not higher than  $\ell$ .

The total number of model terms in the polynomial NARX model given in equation (2) is  $M = (n + \ell)!/[n! \ell!]$ . It can be seen that the full NARX model can include a large number of terms, increasing the risk of overfitting. In addition, only a subset of these terms is typically important to capture the underlying dynamic relationship [2]. Therefore, the canonical-correlation-based fast feature selection is carried out to find out the significant model terms from  $\prod_{k=1}^m x_{i_k}(k)$  with  $y(k)$  as the target. Refer to [20] for details on the specific feature selection steps.

## 2.2 Mini-batch data pruning

For simplicity, the selected model terms are represented by the matrix  $\mathbf{X}$  as follows,

$$\mathbf{X} = \begin{pmatrix} x_{1,1} & \dots & x_{1,N} \\ \vdots & \ddots & \vdots \\ x_{p,1} & \dots & x_{p,N} \end{pmatrix}$$

where  $p$  is the number of the features, that is the selected model terms, and  $N$  is the number of time series samples given the selected features.

A dictionary  $\mathbf{D} \in \mathbb{R}^{p \times K}$  for the matrix  $\mathbf{X} \in \mathbb{R}^{p \times N}$  is obtained by *mini-batch k-means clustering* [25] and used as the target  $\mathbf{Y}$  for the subsequent sample selection step, where  $K$  is the number of atoms in the dictionary, and typically  $K > p$  for an overcomplete dictionary. Each data sample  $\mathbf{x}_j \in \mathbb{R}^p$  (column of  $\mathbf{X}$ ) can be approximated as a sparse

linear combination of the dictionary atoms, given by,

$$\mathbf{x}_j \approx \mathbf{D}\mathbf{a}_j$$

where  $\mathbf{a}_j$  is a sparse coefficient vector for the  $j$ -th sample, which means most of the entries in  $\mathbf{a}_j$  are zero.

The fast selection method based on canonical correlation is performed again, with  $\mathbf{D}$  as the target, to find  $q$  significant samples from the sample matrix  $\mathbf{X}$ . For selection methods which evaluate the linear association between candidates, no additional information is gained when the number of selected samples  $q$  exceeds the rank of the data matrix  $p$ . Therefore, to avoid invalid sample selection due to  $q > p$ , samples are selected in separate batches by the *mini-batch sample selection algorithm*, which is given in Algorithm 1. Within each batch, the redundancy and interaction of samples are considered, while they are ignored between batches.

---

**Algorithm 1:** Mini-batch Sample Selection
 

---

**Input:**  $X \in \mathbb{R}^{p \times N}$  (sample matrix),  $Y \in \mathbb{R}^{p \times K}$  (target matrix),  $q$  (number of samples to select)

**Output:**  $d$  (selected indices)

**Step 1:** Compute the batch size  $b = \lceil q/K \rceil$  and then generate the batch matrix  $B \in \mathbb{R}^{K \times s}$ , where  $B[i, j] \leq b$  and  $\sum B = q$ ;

**Step 2:** Initialize the candidate sample matrix  $X_c \leftarrow X$ ;

**for**  $i \leftarrow 1$  **to**  $K$  **do**

Let  $y_i \leftarrow Y[:, i]$ ;

**for**  $j \leftarrow 1$  **to**  $s$  **do**

**for**  $k \leftarrow 1$  **to**  $B[i, j]$  **do**

Compute the MCC between each column of  $X_c$  and  $y_i$ ;

Select the index  $l^*$  corresponding to the largest MCC;

Append  $l^*$  to  $d$ ;

Remove  $X_c[:, l^*]$  from the candidate matrix;

**return**  $d$ ;

---

### 3 Numerical Case Studis

#### 3.1 Input Data Analysis

Data pruning is crucial in system identification for the following reasons:

1. Firstly, system identification typically involves time-series data sampled from continuous physical processes. When the sampling interval is small, consecutive data points are highly similar, leading to a strong temporal correlation and redundancy. The larger dataset size due to redundant data increases the computational cost of model training.
2. Secondly, the time-shift operation, commonly employed in system identification introduces delayed versions of the signals as new features, which makes the redundancy of the dataset worse. Redundant features do not provide additional information but increase the complexity of the model, making it more prone to overfitting and harder to interpret.

One example is given here to demonstrate this phenomenon intuitively. A time series sampled from  $y(t) = \sin(2\pi t)$  over a duration 1s at a sample rate of 100 Hz is illustrated in Fig. 2. After applying time shifting, the one-dimensional data  $y(t)$  is transformed into two-dimensional data, as shown in Table 1, with a time step of  $\Delta t = 0.01s$ .

The feature-wise redundancy is illustrated in the correlation heatmap of Fig. 3, where the  $i^{th}$  feature corresponds to  $y(t - i\Delta t)$ . The high Pearson's correlation near the main diagonal indicates redundancy between neighbouring features, such as  $y(t - i\Delta t)$  and  $y(t - (i + 1)\Delta t)$ . This kind of redundancy can be mitigated via feature selection.

Fig. 4 shows the redundancy within the time series samples using principal component analysis (PCA). After projecting the 21-dimensional data into two-dimensional space, it is found that the data forms a continuous trajectory over time. The proximity of adjacent samples in the lower-dimensional space given by PCA indicates that there is redundancy between these time series samples. This redundancy can be addressed by data pruning.

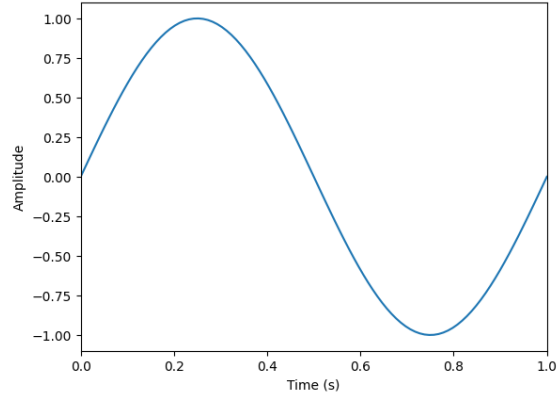


Figure 2: Time series of  $y(t) = \sin(2\pi t)$  at 100 Hz over 1s

$t$ (s)	$y(t)$	$y(t - \Delta t)$	$y(t - 2\Delta t)$	...	$y(t - 20\Delta t)$
0	0	0	0	...	0
0.01	0.063	0	0	...	0
0.02	0.127	0.063	0	...	0
0.03	0.189	0.127	0.063	...	0
0.04	0.251	0.189	0.127	...	0
...	...	...	...	...	...
0.99	-0.000	-0.063	-0.127	...	-0.955

Table 1: Time-shifted data representation with  $\Delta t = 0.01$  s.

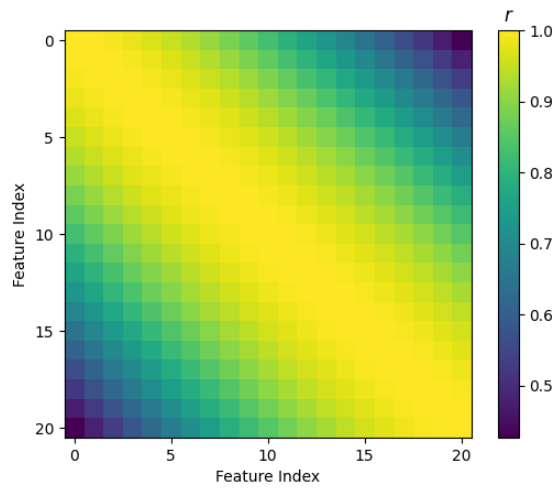


Figure 3: Correlation heatmap illustrating feature-wise redundancy

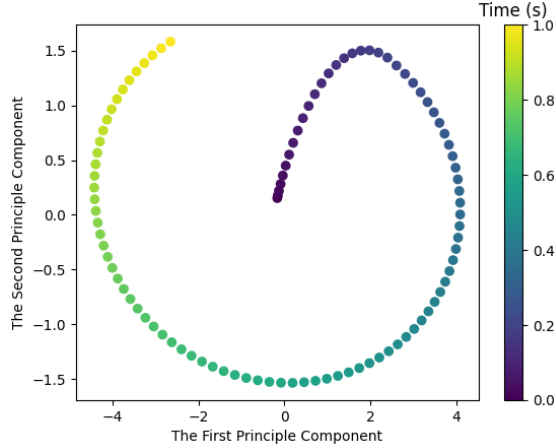


Figure 4: Correlation heatmap illustrating sample-wise redundancy

### 3.2 Data with Dual Stable Equilibria

The simulated time series data is generated by a non-autonomous nonlinear system, given by,

$$\ddot{y} + \dot{y} - y + y^2 + y^3 = u$$

where  $u(t) = 0.1 \cos(0.2\pi t)$ . By setting  $u(t) = 0$  and initialising  $y$  and  $\dot{y}$  with different values, a phase portrait of the nonlinear system is obtained, as shown in Fig. 5.

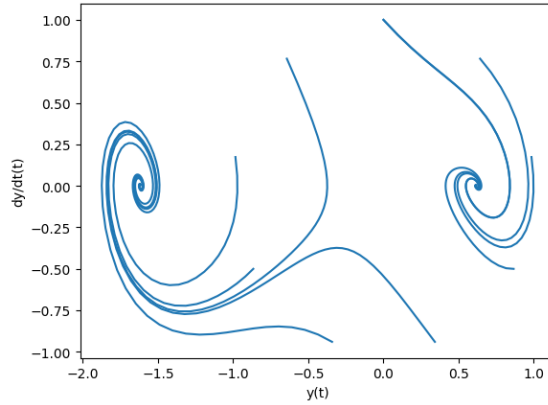


Figure 5: Phase portrait of the nonlinear system with dual stable equilibria

It can be seen that this system exhibits two stable equilibria. To comprehensively capture its dynamics, the data pruning algorithm should identify two distinct types of samples attracted to the different stable spirals and select samples from both categories.

Unlike feature selection, random selection serves as a robust benchmark for sample selection and often outperforms more complex algorithms [26]. Therefore, the results of the proposed data-pruning method will be compared with those of the random selection method to demonstrate its advantages.

The structure of the dual-stable-equilibria (DSE) data is visualized using its first and second principal components. The selected samples and atoms are projected onto these principal directions, with their distribution shown in Fig. 6. It can be found that the samples selected via mini-batch sample selection are distributed across the entire dataset, whereas the randomly selected samples are concentrated primarily on the left and right regions, with less coverage in the middle.

To quantitatively evaluate the selection performance of the mini-batch and random methods, a reduced polynomial NARX model with 10 terms is derived using the full dataset as the baseline. Note that in all case studies, the number

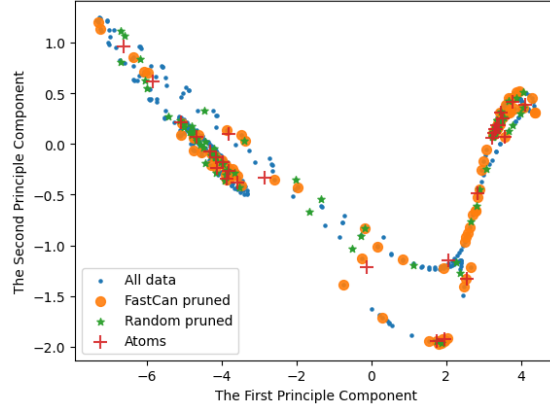


Figure 6: Visualization of the DSE data structure

of terms for system output and input is ten respectively, so the total number of terms is 20, and the degree of polynomial nonlinearity is three. The model coefficients trained on the full dataset are used as the baseline results. The performance of the baseline NARX on the test dataset is provided in Appendix 1. The NARX terms are then fixed, and the model coefficients are trained using the pruned datasets obtained via the mini-batch and random selection methods. The number of atoms for dictionary learning is set to 100, and 600 samples are then selected. The coefficients trained on the two pruned datasets are compared with those from the full dataset using the R-squared. The sample selection and training processes are repeated ten times, with the results presented in Fig. 7.

The mini-batch method gives results with a higher median and lower variance, whereas the random selection method performs significantly worse. The same phenomenon is observed when the number of selected samples varies between 300 and 600, as illustrated in Fig. 8. Furthermore, for the mini-batch method, the variance of the model coefficients decreases as the number of selected samples increases. However, this relationship does not exist when the samples are randomly selected.

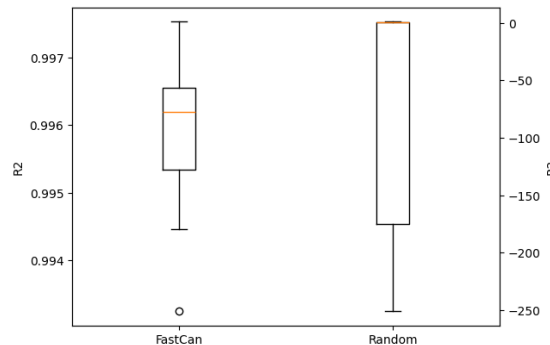


Figure 7: Comparison of sample selection performance between mini-batch and random selection methods on DSE data using R-squared

## 4 Case Studies on the Benchmark Datasets

Two benchmark datasets, collected from the Electro-Mechanical Positioning System (EMPS) [27] and the Wiener-Hammerstein System (WHS) [28] are adopted to evaluate the performance of the mini-batch method for data pruning in real system identification.

### 4.1 Data from the Electro-Mechanical Positioning System

The structure of the data collected from the EMPS, a standard drive configuration for prismatic joints of robots or machine tools, is visualised by its first two principal components, as shown in Fig. 9. The primary nonlinearity of the corresponding data is introduced by friction effects.

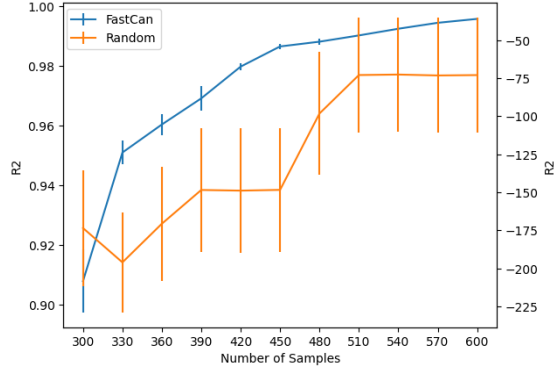


Figure 8: The effect of sample size on the performance of mini-batch and random selection methods for DSE data

The atoms determined for the dictionary learning and the selected samples are also shown in Fig 9. The samples selected by the mini-batch method are spread over all parts of the dataset, while the randomly selected samples are concentrated in the middle two parts but pay less attention to the left and the right parts.

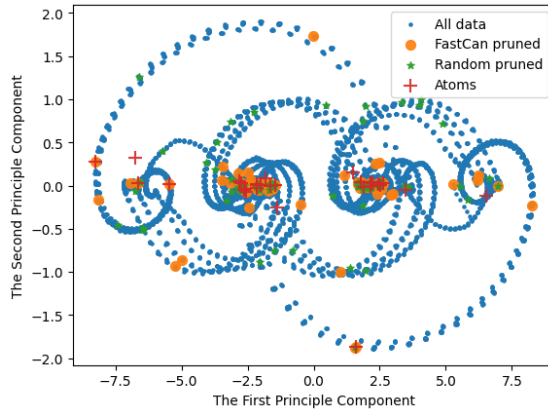


Figure 9: Visualization of the EMPS data structure

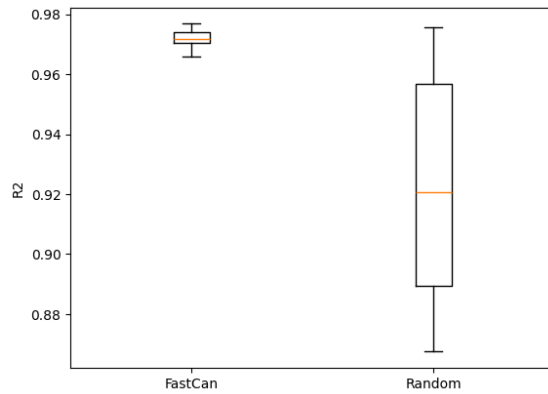


Figure 10: Comparison of sample selection performance between mini-batch and random selection methods on EMPS data using R-squared

The baseline NARX model with 10 terms is derived again, and the model coefficients trained on the full dataset are used as the baseline to quantitatively evaluate the selection performance of the mini-batch and random methods. See Appendix 1 for the performance of the baseline NARX on the test dataset. The number of atoms for dictionary learning is set to 100, and 10000 samples are then selected. The coefficients trained on the two pruned datasets are



compared with those from the full dataset using the R-squared, with the NARX terms fixed. The sample selection and training processes are repeated ten times, with the results illustrated in Fig. 10. In addition, Fig. 11 shows the results corresponding to two methods when the number of selected samples varies between 2000 and 20000.

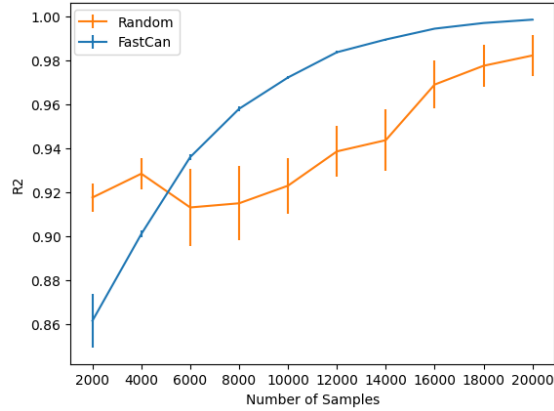


Figure 11: The effect of sample size on the performance of mini-batch and random selection methods for EMPS data

Similar to the observations from the DSE data, the mini-batch method generally produces results with a higher median and lower variance. However, there are exceptions when the number of selected samples is less than 6000, where the randomly selected samples yield higher mean values. This scenario will be analysed and further discussed in Section 4.3. Additionally, as expected, the variance of the model coefficients decreases as the number of selected samples increases.

## 4.2 Data from the Wiener-Hammerstein System

The structure of the data collected from the Wiener-Hammerstein System (WHS), a well-known block-oriented structure consisting of a static nonlinearity between two linear time-invariant blocks, is visualised in Fig. 12 using its first two principal components. The atoms determined for the dictionary learning and the selected samples are also shown in Fig 14. Different from the observations from the DSE data and the EMPS data, the samples obtained by the mini-batch method and random selection method have similar distributions, with the selected samples distributed over the entire dataset.

The same strategy is applied to quantitatively evaluate the sample selection performance of the mini-batch and random methods for the identification task of WHS. The baseline NARX model with 10 terms is derived, and its performance on the test dataset is provided in Appendix 1. The number of atoms for dictionary learning is set to 100, and 10000 samples are selected, with the R-squared results shown in Fig. 13. Then, the number of selected samples varies between 2000 and 20000 to demonstrate the variation of R-squared with the selected sample size, as presented in Fig. 14.

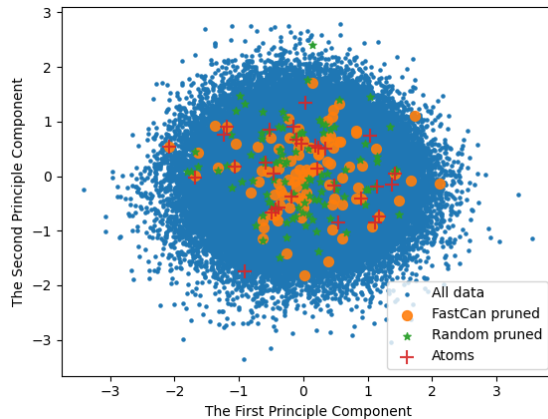


Figure 12: Visualization of the WHS data structure

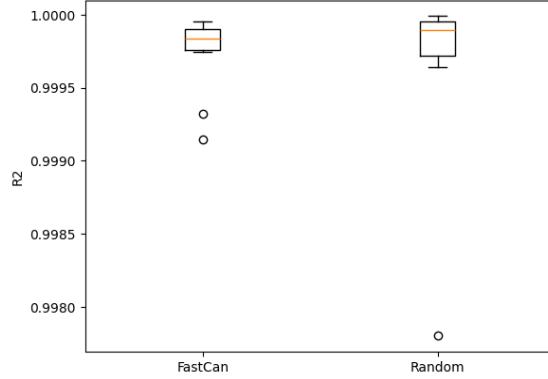


Figure 13: Comparison of sample selection performance between mini-batch and random selection methods on WHS data using R-squared

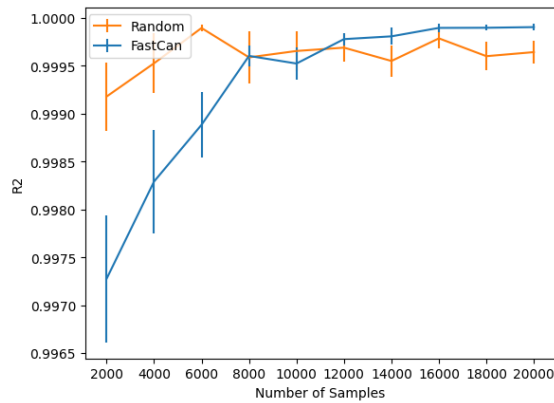


Figure 14: The effect of sample size on the performance of mini-batch and random selection methods for WHS data

Fig. 13 demonstrates that the results obtained by the mini-batch and random methods are similar. This phenomenon is also observed in Fig. 14 when the number of the selected samples exceeds 8000. This result is reasonable and expected, as similar sample distributions provide similar information for system identification. In addition, similar to the EMPS case, when the number of selected samples is small (less than 8000), the randomly selected samples yield higher mean values. This phenomenon will be analysed and further discussed in the following section.

### 4.3 The Effect of Hyperparameters in the Mini-batch Method

In the mini-batch method, sample selection results are influenced by two hyperparameters: the number of atoms in the dictionary and the batch size. To explore how these two hyperparameters affect the performance of the selected samples, system identification results against the varying atom size and batch size for the three previously used datasets are given in Fig. 15 to Fig. 16. For the DSE dataset, 600 samples are selected, while for EMPS and WHS datasets, 10000 samples are selected.

It can be noticed that the batch size in Algorithm 1 is determined by both the number of samples and the number of atoms, with the aim of minimising redundancy among the selected samples when all atoms are used in the sample selection process. Therefore, for the results in Fig. 15, the batch size varies for each atom size. Notably, a larger atom size does not lead to better performance, because some atoms may be learned from noise rather than meaningful data. In Fig. 16, when changing the batch size for each dataset, the number of atoms is fixed at the best atom size obtained from Fig. 15. In this scenario, using a larger batch size to reduce redundancy can improve the performance of the selected samples.

To investigate whether a larger batch size always leads to better selection when the number of atoms is fixed, the relationship between R-squared and batch size for EMPS data with different atom sizes is presented in Fig. 17. The results indicate that the relationship between R-squared and batch size is not a straightforward linear relationship.

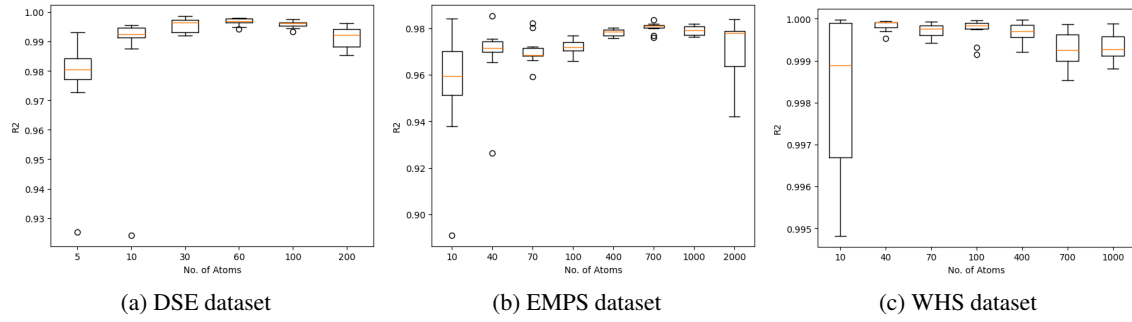


Figure 15: The effect of atom size on the performance of mini-batch method

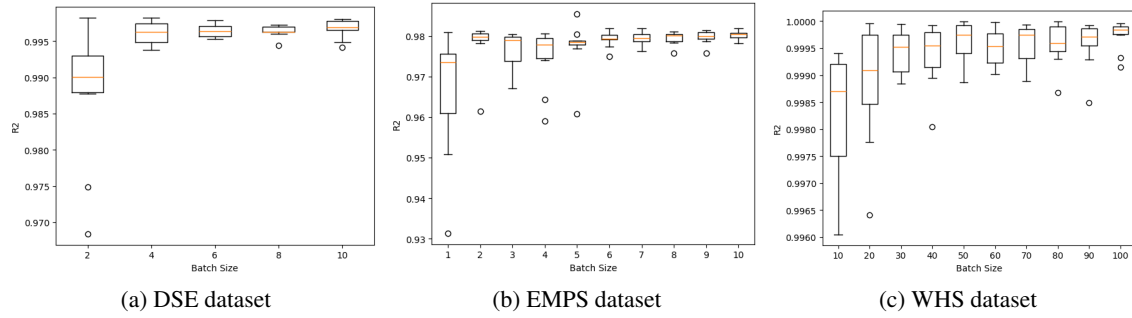


Figure 16: The effect of batch size on the performance of mini-batch method with the best atom size

In summary, the optimal atom size is different for each dataset, and the optimal batch size may not be the ratio of the sample number to the atom size. A more sophisticated method is required to determine the appropriate hyperparameters for the proposed method. Furthermore, the possible reason for the previous-mentioned phenomenon shown in Fig. 11 and Fig. 14 is that when the number of selected samples is small, the performance of the selected samples may be more sensitive to the effectiveness of the hyperparameters.

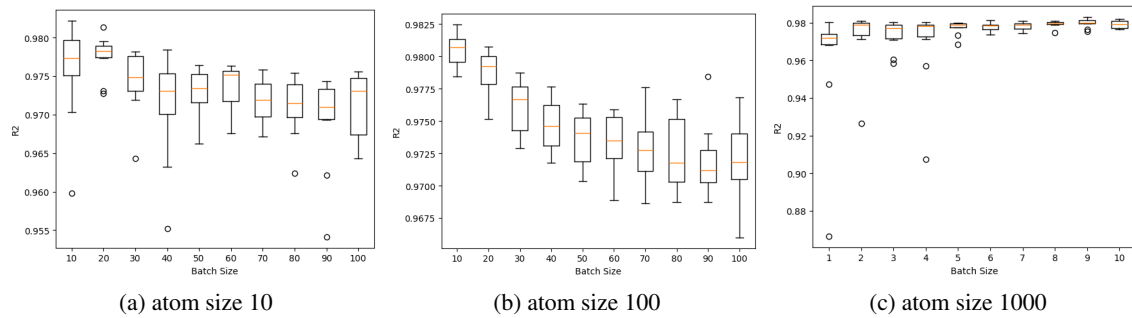


Figure 17: The effect of batch size on the performance of mini-batch method with different atom sizes for EMPS data

## 5 Conclusion

This paper introduces a data-pruning method based on dictionary learning to choose appropriate time-series samples for identification tasks of a discrete system with finite orders. The selection process is independent of the specific system identification technique used.

The case studies on the synthetic and benchmark datasets show that the proposed method effectively reduces the sample size without significantly degrading identification performance. Compared with random selection, the data-pruning method gives better results with a higher mean and lower variance of R-squared values. Additionally, it is found that the careful selection of hyperparameters is crucial, particularly when the number of selected samples is small.

## Appendix 1: Prediction Performance of the Baseline NARX

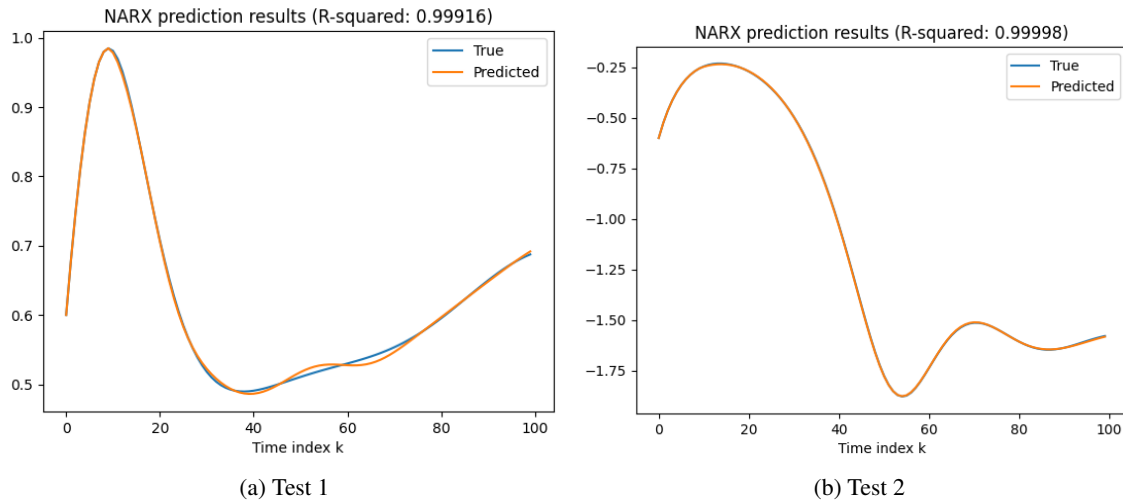


Figure 18: The performance of the baseline NARX model for DSE test data with different initial conditions

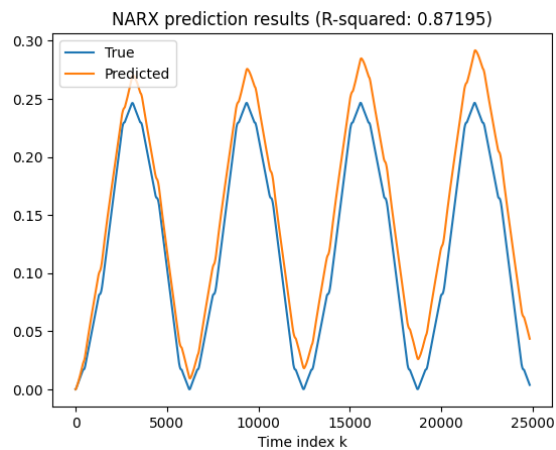


Figure 19: The performance of the baseline NARX model for EMPS test data

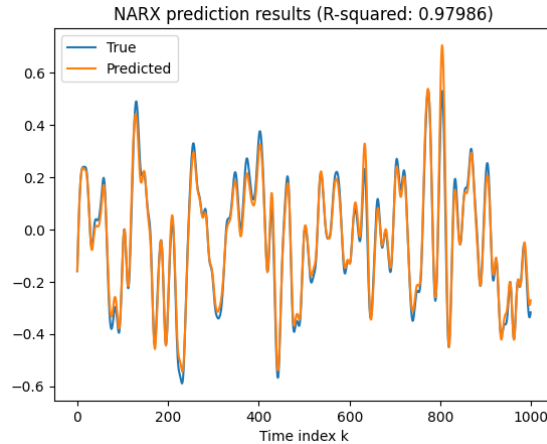


Figure 20: The performance of the baseline NARX model for WHS test data

## References

- [1] George EP Box, Gwilym M Jenkins, Gregory C Reinsel, and Greta M Ljung. *Time Series Analysis: Forecasting and Control (5th ed.)*. John Wiley & Sons, Inc., New Jersey, USA, 2015.
- [2] Stephen A Billings. *Nonlinear System Identification: NARMAX Methods in the Time, Frequency, and Spatio-Temporal Domains*. John Wiley & Sons, Ltd, West Sussex, UK, 2013.
- [3] Oliver Nelles. *Nonlinear System Identification: From Classical Approaches to Neural Networks and Fuzzy Models*. SpringerLink, Berlin, DE, 2001.
- [4] W Thomas Miller, Richard S Sutton, and Paul J Werbos. *Neural Networks for Control*. The MIT Press, London, UK, 1990.
- [5] Gwilym M Jenkins and Donald G Watts. *Spectral Analysis and its Applications*. Holden-Day, Inc., San Francisco, USA, 1968.
- [6] Martin Schetzen. *The Volterra and Wiener Theories of Nonlinear Systems*. John Wiley & Sons Inc., New York, USA, 1980.
- [7] Sheng Chen and Steve A Billings. Representations of non-linear systems: the NARMAX model. *International Journal of Control*, 49(3):1013–1032, 1989.
- [8] Sunil L Kukreja, Henrietta L Galiana, and Robert E Kearney. Narmax representation and identification of ankle dynamics. *IEEE Transactions on Biomedical Engineering*, 50(1):70–81, 2003.
- [9] Richard Boynton, Michael Balikhin, Hualiang Wei, and Ziqiang Lang. Applications of NARMAX in space weather. *Machine learning techniques for space weather*, pages 203–236, 2018.
- [10] Michael Korenberg, Stephen A Billings, YP Liu, and PJ McIlroy. Orthogonal parameter estimation algorithm for non-linear stochastic systems. *International Journal of Control*, 48(1):193–210, 1988.
- [11] Sheng Chen, Stephen A Billings, and Wan Luo. Orthogonal least squares methods and their application to nonlinear system identification. *International Journal of Control*, 50(5):1873–1896, 1989.
- [12] Xia Hong, Richard J Mitchell, Sheng Chen, Chris J Harris, Kang Li, and George W Irwin. Model selection approaches for non-linear system identification: a review. *International Journal of Systems Science*, 39(10):925–946, 2008.
- [13] Graham C Goodwin. Optimal input signals for nonlinear-system identification. In *Proceedings of the Institution of Electrical Engineers*, volume 118, pages 922–926. IET, 1971.
- [14] Raman Mehra. Optimal inputs for linear system identification. *IEEE Transactions on Automatic Control*, 19(3):192–200, 1974.
- [15] Ravi S Raju, Kyle Daruwalla, and Mikko Lipasti. Accelerating deep learning with dynamic data pruning. *arXiv preprint arXiv:2111.12621*, 2021.

- 
- [16] Ben Sorscher, Robert Geirhos, Shashank Shekhar, Surya Ganguli, and Ari S Morcos. Beyond neural scaling laws: beating power law scaling via data pruning. *Advances in Neural Information Processing Systems*, 35:19523–19536, 2022.
  - [17] Zi Yang, Haojin Yang, Soumajit Majumder, Jorge Cardoso, and Guillermo Gallego. Data pruning can do more: A Comprehensive data pruning approach for object re-identification. *arXiv preprint arXiv:2412.10091*, 2024.
  - [18] Max Marion, Ahmet Üstün, Luiza Pozzobon, Alex Wang, Marzieh Fadaee, and Sara Hooker. When less is more: Investigating data pruning for pretraining LLMs at scale. *arXiv preprint arXiv:2309.04564*, 2023.
  - [19] Ruibing Jin, Qing Xu, Min Wu, Yuecong Xu, Dan Li, Xiaoli Li, and Zhenghua Chen. Llm-based knowledge pruning for time series data analytics on edge-computing devices. *arXiv preprint arXiv:2406.08765*, 2024.
  - [20] Sikai Zhang, Tingna Wang, Keith Worden, Limin Sun, and Elizabeth J Cross. Canonical-correlation-based fast feature selection for structural health monitoring. *Mechanical Systems and Signal Processing*, 223:111895, 2025.
  - [21] Michal Aharon, Michael Elad, and Alfred Bruckstein. K-svd: An algorithm for designing overcomplete dictionaries for sparse representation. *IEEE Transactions on Signal Processing*, 54(11):4311–4322, 2006.
  - [22] Julien Mairal, Francis Bach, and Jean Ponce. Task-driven dictionary learning. *IEEE Transactions on Pattern Analysis and Machine Intelligence*, 34(4):791–804, 2011.
  - [23] Tiep Huu Vu and Vishal Monga. Fast low-rank shared dictionary learning for image classification. *IEEE Transactions on Image Processing*, 26(11):5160–5175, 2017.
  - [24] Simon Billinge. bg-mpl-stylesheets. <https://github.com/Billingegroup/bg-mpl-stylesheets>, 2024.
  - [25] David Sculley. Web-scale k-means clustering. In *Proceedings of the 19th international conference on World wide web*, pages 1177–1178, 2010.
  - [26] Fadhel Ayed and Soufiane Hayou. Data pruning and neural scaling laws: fundamental limitations of score-based algorithms. *arXiv preprint arXiv:2302.06960*, 2023.
  - [27] Alexandre Janot, Maxime Gautier, and Mathieu Brunot. Data set and reference models of EMPS. In *Nonlinear System Identification Benchmarks*, 2019.
  - [28] Johan Schoukens and Lennart Ljung. Wiener-hammerstein benchmark. Technical report, Linköping University Electronic Press, 2009.